

siRNA targeting the NS5B region reduced luciferase expression from the chimaeric HCV NS5B protein–luciferase fusion by 75% ($\pm 6.8\%$; 6 animals per group). This result suggests that it may be feasible to use RNAi as a therapy against other important human pathogens.

Although our results show that siRNAs are functional in mice, delivery remains a major obstacle. Unlike siRNAs, functional small-hairpin RNAs (shRNAs) can be expressed *in vivo* from DNA templates using RNA polymerase III promoters^{8,9}; they are as effective as siRNAs in inducing gene suppression. Expression of a cognate shRNA (pShh1-Ff1; see supplementary information) inhibited luciferase expression by up to 98% ($\pm 0.6\%$), with an average suppression of 92.8% ($\pm 3.39\%$) in three independent experiments (Fig. 1c, d). An empty shRNA-expression vector had no effect (results not shown); reversing the orientation of the shRNA (pShh1-Ff1rev) insert prevents gene silencing because it alters the termination by RNA polymerase III and generates an improperly structured shRNA. These findings indicate that plasmid-encoded shRNAs can induce a potent and specific RNAi response in adult mice.

RNAi may find application in functional genomics or in identifying targets for designer drugs. It is a more promising system than gene-knockout mice because groups of genes can be simultaneously rendered ineffective without the need for time-consuming crosses. Gene therapy currently depends on the ectopic expression of exogenous proteins; however, RNAi may eventually complement this gain-of-function approach by silencing disease-related genes with DNA constructs that direct the expression of shRNAs. Our method of RNAi delivery could also be tailored to take advantage of developing viral and non-viral gene-transfer vectors in a clinical context.

Anton P. McCaffrey*, **Leonard Meuse***, **Thu-Thao T. Pham***, **Douglas S. Conklin†**, **Gregory J. Hannon†**, **Mark A. Kay***

*Departments of Pediatrics and Genetics, Stanford University School of Medicine, Stanford, California 94305-5208, USA
e-mail: markay@stanford.edu

†Cold Spring Harbor Laboratory, 1 Bungtown Road, Cold Spring Harbor, New York 11724, USA

1. Elbashir, S. M. *et al.* *Nature* **411**, 494–498 (2001).
2. Zhang, G., Budker, V. & Wolff, J. A. *Hum. Gene Therapy* **10**, 1735–1737 (1999).
3. Liu, F., Song, Y. & Liu, D. *Gene Therapy* **6**, 1258–1266 (1999).
4. Chang, J., Sigal, L. J., Lerro, A. & Taylor, J. J. *Virology* **75**, 3469–3473 (2001).
5. Contag, C. H. *et al.* *Photochem. Photobiol.* **66**, 523–531 (1997).
6. Yant, S. R. *et al.* *Nature Genet.* **25**, 35–41 (2000).
7. Bitko, V. & Barik, S. *BMC Microbiol.* **1**, 34 (2001).
8. Paddison, P. J., Caudy, A. A., Bernstein, E., Hannon, G. J. & Conklin, D. S. *Genes Dev.* **16**, 948–958 (2002).
9. Tuschl, T. *Nature Biotechnol.* **20**, 446–448 (2002).

Supplementary information accompanies this communication on Nature's website.

Competing financial interests: declared none.

COMMUNICATIONS ARISING

Orbital physics

Experimental quest for orbital waves

One challenge in condensed-matter physics is the experimental confirmation of a new kind of elementary excitation — orbital waves, or orbitons, which are predicted to exist in an orbitally ordered state. Saitoh *et al.*¹ have observed three peaks at 160, 144 and 126 meV in the Raman scattering of orbitally ordered lanthanum manganate (LaMnO₃), and interpret these as evidence of orbitons. However, we find similar peaks in the optical conductivity, $\sigma(\omega)$, of LaMnO₃ and point out that the direct observation of orbitons in $\sigma(\omega)$ is prohibited by a selection rule. This suggests that the Raman peaks observed by Saitoh *et al.* arise from multiphonons, and that the existence of orbitons has yet to be experimentally confirmed.

We determined $\sigma(\omega)$ by measuring both the transmittance and reflectance of single crystals, using a sample polished to a thickness of $d \approx 62 \mu\text{m}$ for the former. We com-

pared $\sigma(\omega)$ of LaMnO₃ with the Raman data of Saitoh *et al.*¹ and found that the peaks in $\sigma(\omega)$ were similar to the Raman features (Fig. 1, top), albeit with slightly different frequencies (160, 146, 130 and 118 meV).

The orbital excitations discussed by Saitoh *et al.* involve transitions between orbital states of the same parity. These transitions do not contribute directly to $\sigma(\omega)$ owing to the parity selection rule; that is, they are not infrared-active. They may become weakly infrared-active in the presence of defects or by the simultaneous excitation of a parity-breaking Mn–O bond-stretching phonon². The latter, phonon-activated mechanism is the more effective way to break the selection rule. Stronger features are therefore expected in $\sigma(\omega)$ at frequencies that — compared to the Raman peaks — are shifted by the respective phonon frequency of about 70 meV. As this is not the case, the peaks in $\sigma(\omega)$ cannot be explained by orbitons, challenging the orbiton interpretation of the Raman data.

We suggest that all peaks should be interpreted as arising from multiphonons. The sharp increase in $\sigma(\omega)$ at low frequen-

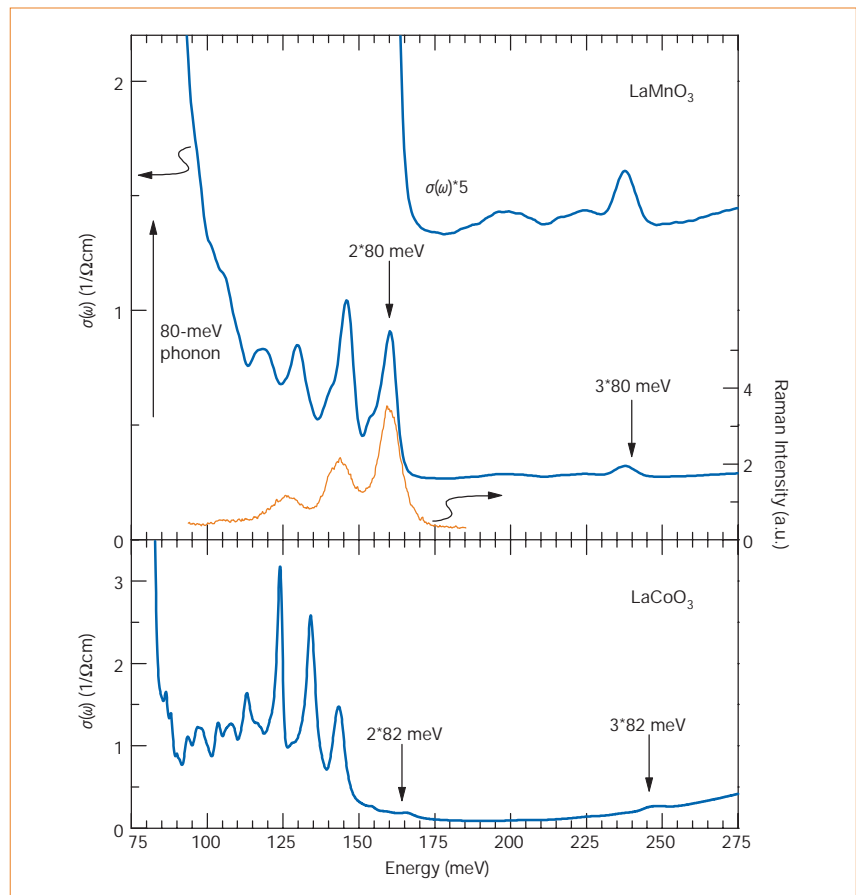


Figure 1 Optical conductivity $\sigma(\omega)$ of LaMnO₃ and LaCoO₃, and Raman measurements on LaMnO₃ at a temperature of 4 K. Top, comparison of $\sigma(\omega)$ (thick blue line) and Raman intensity (from Saitoh *et al.*¹; thin yellow line) of LaMnO₃ reveals a close similarity between the two spectra. In $\sigma(\omega)$ the highest peaks of single-, two- and three-phonon absorption are observed at 80, 160 and 240 meV, respectively. Inset, enlargement of the three-phonon range of $\sigma(\omega)$. Bottom, $\sigma(\omega)$ of LaCoO₃, showing multiphonon peaks, for example at 282 and 382 meV.

cies indicates the upper limit of (single) phonon absorption. The highest infrared-active phonon peak is observed at 80 meV (ref. 3), showing that the peaks at 160 and 240 meV are within the range of two- and three-phonon absorption, respectively. By increasing the number of phonons involved in the absorption process from one to two to three, the spectral weight in $\sigma(\omega)$ is reduced each time by one to two orders of magnitude. Moreover, multiphonon Raman scattering is predicted⁴ to be particularly strong in orbitally ordered LaMnO₃.

The multiphonon features do not necessarily correspond to simple multiples of the $k=0$ single-phonon peaks observed in Raman or $\sigma(\omega)$, because phonon modes from the entire Brillouin zone can be combined to yield the required total momentum, $k_{\text{tot}}=0$. The multiphonon peaks reflect peaks in the combined density of states weighted for each technique by the respective matrix element. In LaMnO₃, Raman and infrared spectroscopy are sensitive to excitations of different symmetry, which explains the slightly different peak frequencies observed using the two methods.

Below about 160 meV, multiphonon features are common in transition-metal oxides that have pseudocubic, perovskite structures. As an example, Fig. 1 shows $\sigma(\omega)$ for LaCoO₃, for which we measured the transmittance on a single crystal with $d \approx 37 \mu\text{m}$. At a temperature of 4 K, LaCoO₃ is in a non-magnetic state ($t_{2g}^6 e_g^0$) without orbital degeneracy or orbital order, and so orbital waves can be excluded as the origin of the observed peaks. These features must also be interpreted as arising from multiphonons.

Finally, we note that the peak frequencies are rather low for orbitons. Two components contribute to the orbiton energy: one is purely electronic and the other is due to electron-phonon coupling. Saitoh *et al.*¹ predict on theoretical grounds that the electronic contribution to the highest peak should be about $4J_1 \approx 200$ meV, and assume that the electron-phonon contribution is rather small ($0.56J_1 \approx 28$ meV). However, other estimates of the electron-phonon contribution⁵⁻¹¹ vary between 0.7 and 2.0 eV and therefore do not support the existence of orbitons at 160 meV.

We conclude that the observed features of $\sigma(\omega)$ are due to multiphonons, and see no evidence so far to support an alternative explanation of the similar Raman peaks. Raman measurements on an oxygen-isotope-substituted sample of LaMnO₃ should clarify this point.

M. Grüninger*, **R. Rückamp***, **M. Windt***, **P. Reutler†‡**, **C. Zobel***, **T. Lorenz***, **A. Freimuth***, **A. Revcolevschi‡**

*2 Physikalisches Institut, Universität zu Köln, 50937 Köln, Germany

e-mail: grueninger@ph2.uni-koeln.de

†RWTH-Aachen, 52056 Aachen, Germany

‡Laboratoire de Physico-Chimie de l'Etat Solide, Université Paris-Sud, 91405 Orsay, France

1. Saitoh, E. *et al.* *Nature* **410**, 180–183 (2001).
2. Ballhausen, C. J. *Introduction to Ligand Field Theory* (McGraw-Hill, New York, 1962).
3. Paolone, A. *et al.* *Phys. Rev. B* **61**, 11255–11258 (2000).
4. Perebeinos, V. & Allen, P. B. *Phys. Rev. B* **64**, 085118 (2001).
5. Millis, A. J. *Phys. Rev. B* **53**, 8434–8441 (1996).
6. Pickett, W. E. & Singh, D. J. *Phys. Rev. B* **53**, 1146–1160 (1996).
7. Solov'ev, I., Hamada, N. & Terakura, K. *Phys. Rev. B* **53**, 7158–7170 (1996).
8. Elfmov, I. S., Anisimov, V. I. & Sawatzky, G. A. *Phys. Rev. Lett.* **82**, 4264–4267 (1999).
9. Allen, P. B. & Perebeinos, V. *Phys. Rev. Lett.* **83**, 4828–4831 (1999).
10. Ahn, K. H. & Millis, A. J. *Phys. Rev. B* **61**, 13545–13559 (2000).
11. Bala, J. & Oles, A. M. *Phys. Rev. B* **62**, R6085–R6088 (2000).

Saitoh et al. reply — We disagree with the assertion of Grüninger *et al.* that the Raman peaks from LaMnO₃, which we interpret as being due to scattering from orbital excitation, are caused by multiphonon excitation.

First, the estimated oscillator strength, f , of their observed 160-meV peak in the optical conductivity, $\sigma(\omega)$, is less than 1×10^{-6} , which is much weaker than those of the main Mn–O stretching mode at 71 meV ($f \approx 2 \times 10^{-4}$) and of the electronic charge excitation at around 1.9 eV ($f \approx 2.7 \times 10^{-1}$; ref. 1). Such a weak infrared peak is explained by a spin-allowed d – d electronic excitation that becomes infrared-active through the disruption of local-inversion symmetry due to impurities and/or defects. The orbiton represents one such low-energy d – d excitation, although it can show k -dispersion.

Figure 1 shows the polarization dependence of the $\sigma(\omega)$ and Raman spectra for a detwinned LaMnO₃ crystal at about 10 K. As the $\sigma(\omega)$ was deduced from the reflectivity, the weak intensity (around $1 \Omega^{-1} \text{cm}^{-1}$) of the infrared-active peak is barely detectable. The $\sigma(\omega)$ spectra are also plot-

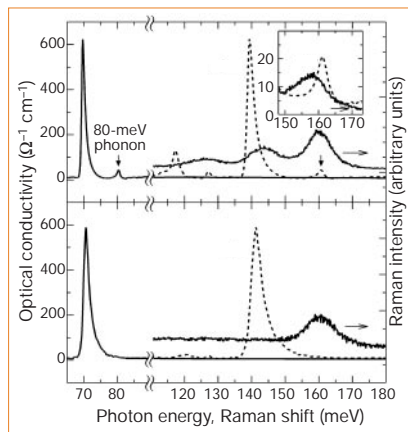


Figure 1 Polarized optical conductivity $\sigma(\omega)$ and Raman spectra in a detwinned LaMnO₃ crystal at around 10 K (inset, Raman spectrum at 300 K). Top, $E_{\perp z}$ spectra, (x,x) configuration; bottom, $E_{\parallel z}$ spectra, (z,z) configuration. The $\sigma(\omega)$ spectra are also plotted as functions of the doubled photon energy (dashed lines).

ted as functions of the doubled photon energy (Fig. 1, dashed lines). The infrared-active phonon at 80 meV is observed only in the $E_{\perp z}$ polarization ((x,x) configuration; Fig. 1, top). The $E_{\parallel z}$ spectra do not show any peak at the corresponding energy, although the prominent Raman band at 160 meV is evident in the (z,z) configuration (Fig. 1, bottom).

Any combination of two infrared-active modes with the same symmetry may produce the Raman-active symmetry. However, it is hard to reconcile a two-phonon interpretation in terms of an 80-meV in-plane-active mode, with the strong Raman intensity observed in the (z,z) configuration. In addition, the peak energy of the Raman band in the (x,x) configuration deviates from the doubled energy of the 80-meV phonon peak with increasing temperature (Fig. 1, inset).

In LaMnO₃, the 80-meV infrared-active mode in the $E_{\perp z}$ spectrum disappears above $T_{\text{IT}} \approx 750$ K. In LaCoO₃, the $\sigma(\omega)$ spectra deduced from the reflectivity data do not show any prominent peak near 82 meV (ref. 2), in contrast to the 80-meV mode in LaMnO₃, which is weak but clearly discerned as the Jahn–Teller (JT) distortion-induced mode ($f \approx 1 \times 10^{-5}$). The origin of the 82-meV peak in LaCoO₃ observed by Grüninger *et al.* is interesting, but irrelevant to the origin of the intense, high-frequency Raman modes observed for LaMnO₃.

By considering both the electronic and phononic contributions to the orbiton energy equally, we have quantitatively estimated the parameter values of the interactions³. Using these values, we have calculated the Raman spectra that show good agreement with the experimental results. The large discrepancy between our and previous estimates, as pointed out by Grüninger *et al.*, arises from the absence or averaged treatment of the strong electron correlation.

E. Saitoh*, **S. Okamoto†**, **K. Tobe‡**, **K. Yamamoto§**, **T. Kimura‡**, **S. Ishihara‡**, **S. Maekawa||**, **Y. Tokura‡**

*Department of Physics, Keio University, Yokohama 223-8522, Japan

†Institute of Physical and Chemical Research (RIKEN), Saitama 351-0198, Japan

‡Department of Applied Physics, University of Tokyo, Tokyo 113-8656, Japan e-mail: tokura@ap.t.u-tokyo.ac.jp

§Photodynamics Research Center, RIKEN, Sendai 980-0845, Japan

||Institute for Materials Research, Tohoku University, Sendai 980-8577, Japan

1. Tobe, K., Kimura, T., Okimoto, Y. & Tokura, Y. *Phys. Rev. B* **64**, 184421 (2001).
2. Yamaguchi, S., Okimoto, Y. & Tokura, Y. *Phys. Rev. B* **55**, R8666–R8669 (1997).
3. Okamoto, S., Ishihara, S. & Maekawa, S. *Phys. Rev. B* **65**, 144403 (2002).